

Depletion of microglia with PLX3397 attenuates MK-801-induced hyperactivity associated with regulating inflammation-related genes in the brain

Rong-Jun Ni^{1,2,#}, Yi-Yan Wang^{1,2,#}, Tian-Hao Gao^{1,2}, Qi-Run Wang^{1,2}, Jin-Xue Wei^{1,2}, Lian-Sheng Zhao^{1,2}, Yang-Rui Ma³, Xiao-Hong Ma^{1,2,*}, Tao Li^{4,5,6,*}

¹ Mental Health Center and Psychiatric Laboratory, West China Hospital, Sichuan University, Chengdu, Sichuan 610041, China

² Sichuan Clinical Medical Research Center for Mental Disorders, Chengdu, Sichuan 610044, China

³ Golden Apple Jincheng NO.1 Secondary School, Chengdu, Sichuan 610213, China

⁴ Affiliated Mental Health Center & Hangzhou Seventh People's Hospital, Zhejiang University School of Medicine, Hangzhou, Zhejiang 310013, China

⁵ NHC and CAMS Key Laboratory of Medical Neurobiology, MOE Frontier Science Center for Brain Science and Brain-machine Integration, School of Brain Science and Brain Medicine, Zhejiang University, Hangzhou, Zhejiang 310014, China

⁶ Guangdong-Hong Kong-Macao Greater Bay Area Center for Brain Science and Brain-Inspired Intelligence, Guangzhou, Guangdong 510799, China

ABSTRACT

Acute administration of MK-801 (dizocilpine), an N-methyl-D-aspartate receptor (NMDAR) antagonist, can establish animal models of psychiatric disorders. However, the roles of microglia and inflammation-related genes in these animal models of psychiatric disorders remain unknown. Here, we found rapid elimination of microglia in the prefrontal cortex (PFC) and hippocampus (HPC) of mice following administration of the dual colony-stimulating factor 1 receptor (CSF1R)/c-Kit kinase inhibitor PLX3397 (peixidartinib) in drinking water. Single administration of MK-801 induced hyperactivity in the open-field test (OFT). Importantly, PLX3397-induced depletion of microglia prevented the hyperactivity and schizophrenia-like behaviors induced by MK-801. However, neither repopulation of microglia nor inhibition of microglial activation by minocycline affected MK-801-induced hyperactivity. Importantly, microglial density in the PFC and HPC was significantly correlated with behavioral changes. In addition, common and distinct glutamate-, GABA-, and inflammation-related gene (116 genes) expression patterns were observed in the brains of PLX3397- and/or MK-801-treated mice. Moreover, 10 common inflammation-related genes (*CD68*, *CD163*, *CD206*, *TMEM119*, *CSF3R*, *CX3CR1*, *TREM2*, *CD11b*, *CSF1R*, and *F4/80*) with very strong correlations were

identified in the brain using hierarchical clustering analysis. Further correlation analysis demonstrated that the behavioral changes in the OFT were most significantly associated with the expression of inflammation-related genes (*NLRP3*, *CD163*, *CD206*, *F4/80*, *TMEM119*, and *TMEM176a*), but not glutamate- or GABA-related genes in PLX3397- and MK-801-treated mice. Thus, our results suggest that microglial depletion via a CSF1R/c-Kit kinase inhibitor can ameliorate the hyperactivity induced by an NMDAR antagonist, which is associated with modulation of immune-related genes in the brain.

Keywords: Microglia; Psychiatric disorders; Prefrontal cortex; Hippocampus; Immunity; Colony-stimulating factor 1 receptor

INTRODUCTION

Rodent models of schizophrenia can be established through

Received: 18 December 2022; Accepted: 28 April 2023; Online: 04 May 2023

Foundation items: This work was supported by the National Natural Science Foundation of China (81920108018, 82230046, 82001432), Ministry of Science and Technology of the People's Republic of China (2022ZD0211700, 2022ZD0205200), Natural Science Foundation of Sichuan Province (2022NSFSC1607), Key Research and Development Program of Science and Technology Department of Sichuan Province (22ZDYF1531, 22ZDYF1696), Key R & D Program of Zhejiang (2022C03096), Special Foundation for Brain Research from Science and Technology Program of Guangdong (2018B030334001), China Postdoctoral Science Foundation (2020TQ0213, 2020M683319), and Sichuan University (2022SCUH0023)

*Authors contributed equally to this work

*Corresponding authors, E-mail: maxiaohong@scu.edu.cn; litaozjusc@zju.edu.cn

This is an open-access article distributed under the terms of the Creative Commons Attribution Non-Commercial License (<http://creativecommons.org/licenses/by-nc/4.0/>), which permits unrestricted non-commercial use, distribution, and reproduction in any medium, provided the original work is properly cited.

Copyright ©2023 Editorial Office of Zoological Research, Kunming Institute of Zoology, Chinese Academy of Sciences

acute administration of MK-801 (dizocilpine), an N-methyl-D-aspartate receptor (NMDAR) antagonist (Chen et al., 2022; Svoboda et al., 2015). Many studies have shown that acute MK-801 administration can induce hyperlocomotion, stereotypy, and ataxia in mice and establish animal models of psychiatric disorders (Bradford et al., 2010; Chen et al., 2022). Psychiatric disorders are often accompanied by motor abnormalities and abnormal functional connectivity in the prefrontal cortex (PFC) and hippocampus (HPC) (Walther et al., 2017; Wegrzyn et al., 2022).

Postmortem examination of psychiatric patient brains found an increase in microglial cell densities and a decrease in microglial arborization (Gober et al., 2022). In clinical trials, postmortem transcriptional profiling of schizophrenia revealed increased expression of immune-related genes in the PFC and HPC (Hwang et al., 2013; Lanz et al., 2019). Furthermore, recent evidence has shown that microglial disturbances and abnormal changes in inflammation-related gene expression are involved in the pathology of psychiatric disorders, including schizophrenia and depression (Gober et al., 2022; Lanz et al., 2019; Volk, 2017). However, the neural support and neuroprotection of microglia and inflammation-related genes in psychiatric disorders remain unknown.

Colony-stimulating factor 1 receptor (CSF1R) signaling is necessary for microglial homeostasis and neuronal survival in the adult brain (Elmore et al., 2014). A previous study on *Csf1r* mutant zebrafish revealed that CSF1R regulates microglial density and distribution but not microglial differentiation in the brain (Oosterhof et al., 2018). PLX3397 (pexidartinib) and PLX5622, dual CSF1R/c-Kit kinase inhibitors, have been widely used to eliminate microglia in the brain and macrophages in the peripheral tissues of rodents through diet, oral gavage, or intraperitoneal (i.p.) injection (Chen et al., 2022; Elmore et al., 2014; Ma et al., 2020; Najafi et al., 2018). Microglia can repopulate to normal levels within 7 days of pharmacologically induced depletion (Elmore et al., 2014). Moreover, administration of a CSF1R/c-Kit kinase inhibitor decreases the expression of inflammation-related genes and proteins in the central and peripheral systems (Elmore et al., 2014; Lei et al., 2020; Vichaya et al., 2020). However, little is known about the effects of the CSF1R/c-Kit kinase inhibitor PLX3397 on MK-801-induced hyperactivity in mice.

Here, we investigated the effects of depletion, repopulation (forced microglial turnover using PLX3397), and minocycline-mediated inhibition of microglia on MK-801-induced hyperactivity in mice. In addition, we explored the correlation between hyperactivity and microglial density controlled by PLX3397 treatment. Furthermore, we evaluated the effects of PLX3397 and MK-801 administration on glutamate-, GABA-, and inflammation-related gene expression profiles in the PFC and HPC. Finally, we determined the correlations among glutamate-, GABA-, and inflammation-related gene expression levels and MK-801-induced behaviors.

MATERIALS AND METHODS

Animals

Eight-week-old male C57BL/6 mice were purchased from the Chengdu Dossy Experimental Animals Company (Sichuan, China). All mice were group-housed in an animal facility under a 12 h light/dark cycle (lights on at 0800h), with food and water available *ad libitum*. All study protocols were approved by the Animal Care and Use Committee of Sichuan University

(Approval No.: 2019044A). All efforts were made to minimize animal suffering and reduce the number of animals used.

Drug administration

Pexidartinib (PLX3397, MedChemExpress, Cat# HY-16749, USA) was dissolved in 2% dimethyl sulfoxide (DMSO), 0.1% Tween 80, and 5% sulfobutylether- β -cyclodextrin (SBE- β -CD). PLX3397 was administered orally in drinking water at 1 mg/mL (delivering daily doses of approximately 150 mg/kg body weight). Control mice received vehicle solution (2% DMSO/0.1% Tween 80/5% SBE- β -CD/93% water, vol/vol/vol). All mice were habituated to drink the vehicle solution *ad libitum* for 5 days prior to exposure to the PLX3397 solution. Drinking bottles were filled daily with newly prepared PLX3397 and vehicle solutions. All drinking bottles were manually shaken once a day for a few seconds. Alternatively, PLX3397 was administered (i.p. injection) in mice at a dose of 50 mg/kg (12 h intervals). Minocycline (MedChemExpress, Cat# HY-17412, USA) was dissolved in sterile saline and injected (i.p.) at a dose of 50 mg/kg. The animals were injected twice a day with either minocycline or saline for 3 consecutive days before behavioral testing. MK-801 (Sigma-Aldrich, USA, Cat# M107) was freshly prepared in sterile saline and injected (i.p.) at a volume of 0.01 mg/mL. MK-801 (0.1 mg/kg body weight) was given to each mouse 30 min before behavioral testing. Control experiments were performed following saline administration. Administration of PLX3397 and minocycline was stopped 12 h before behavioral testing.

Behavioral testing

Before behavioral testing, all mice were handled by the experimenter for 1 min per day for 3 days to allow them to habituate to experimental manipulation. On the day of testing, mice were allowed to acclimate to the behavioral testing room for 1 h prior to behavioral testing. The mice were tested successively using the open-field test (OFT) 30 min after MK-801 administration and elevated plus-maze (EPM) test 5 min after the OFT. All tests were performed between 0900h and 1700h under dim light. The recorded videos were analyzed using EthoVision (v12.0) tracking software (Noldus, Netherlands).

Open-field test: At 30 min after MK-801 administration, the mice were subjected to the OFT to evaluate locomotor exploration, as described previously (Ni et al., 2020, 2022). The open-field apparatus was a square arena (40 cm \times 40 cm \times 35 cm) consisting of a white Plexiglas box. Each mouse was placed in the corner and permitted to freely explore the apparatus for 5 min. After each test, the apparatus was cleaned with 75% alcohol to remove any trace of odor. During the 5 min test period, total distance moved, time spent in the center zone, and number of center entries in the OFT were analyzed using the video tracking system.

Elevated plus-maze test: The mice were subjected to the EPM to evaluate anxiety-related behavior, as described previously (Ni et al., 2020, 2022). The EPM was constructed of a white Plexiglas box with two open arms (30 cm \times 7 cm, length \times width) and two closed arms (30 cm \times 7 cm \times 16 cm, length \times width \times height). The maze contained two opposite closed and open arms set in a plus-shaped configuration elevated 60 cm above the ground. A video camera was fixed above the EPM to record movements for analysis. The mice were individually placed in the center of the maze facing one of the closed arms, and allowed to freely explore the apparatus for 5 min. After each test, the apparatus was

cleaned with 75% alcohol to remove any trace of odor. During the 5 min test period, the video tracking system was used to quantify total distance moved, number of arm entries, and time spent in the open arms.

Prepulse inhibition of startle reflex (PPI): Mice were injected with either MK-801 or saline 30 min before the PPI test. Each mouse was placed into a startle apparatus (Med Associates Inc., Model ENV-022S, USA) and the PPI test was conducted as described previously, with several modifications (Nguyen et al., 2014). A 64 dB background noise was set throughout the PPI test. The PPI test session consisted of Block 1 (10 sequential 120 dB trials), Block 2 (40 pseudorandomized startle trials), and Block 3 (10 sequential 120 dB trials). The pseudorandomized startle trials in Block 2 consisted of one of the following five trials: one pulse-alone trial (120 dB), three prepulse-pulse trials (74, 78, or 86 dB, followed 100 ms later by a 40 ms, 120 dB noise burst), and one no-stimulus trial (background noise). Trials were performed with an intertrial interval of 10–20 s. The percentage PPI for each acoustic prepulse trial type was calculated as follows: (mean startle amplitude of pulse-alone trials–startle amplitude of prepulse-pulse trial)/mean startle amplitude of pulse-alone trials×100).

Tissue preparation

One day after behavioral testing or final treatment, the mice ($n=82$) were anesthetized using isoflurane (4% for induction and 2% for maintenance, RWD, Shenzhen, China) and perfused transcardially with 0.9% saline followed by 4% paraformaldehyde (PFA) in phosphate buffer (0.1 mol/L, pH 7.4). After perfusion, the brains were removed and postfixed by immersion in 4% PFA overnight at 4 °C. The brains were then transferred to 15% sucrose in phosphate-buffered saline (PBS; 0.1 mol/L, pH 7.4), until the tissues sank, followed by 30% sucrose in PBS. Tissues were frozen and sectioned (40 μ m) on a cryostat (Minux FS800A, RWD Inc., China), then stored in cryoprotectant (ethylene glycol, glycerol, and PBS, 3:3:4 by volume; pH 7.4) at –20 °C until use.

Immunohistochemistry

Specificity of the rabbit anti-ionized calcium-binding adaptor molecule 1 primary antibody (Iba1; #019-19741, Japan, RRID: AB_839504) has been previously confirmed in rodents (Vanryzin et al., 2021; Zhao et al., 2019). A series of brain sections was taken from the PLX3397- and MK-801-treated mice (240 μ m intervals). These sections were processed for immunohistochemical analysis of Iba1 (microglial marker), as described previously (Ni et al., 2014). Briefly, the free-floating sections were rinsed in PBS and treated with 0.3% hydrogen peroxide (H₂O₂) and 0.3% Triton X-100 in PBS for 30 min to quench endogenous peroxidase activity. After incubation with 5% normal goat serum (Solarbio, China) in PBST (PBS containing 0.3% Triton X-100) for 30 min, the free-floating sections were immunoreacted with rabbit anti-Iba1 antibody (Wako, #019-19741, at 1:1 000 dilution, RRID: AB_839504) in PBST containing 5% normal goat serum at 4 °C overnight. Signal amplification was performed with biotinylated goat anti-rabbit immunoglobulin G (IgG) (at 1:200 dilution, Vector Laboratories, USA) in PBST at 37 °C for 1 h and avidin-biotin peroxidase complex (at 1:200 dilution, Vector Laboratories, USA) in PBST at 37 °C for 1 h. Finally, chromogen development was performed with 0.05% diaminobenzidine (Sigma-Aldrich, USA) in PBST containing 0.03% H₂O₂ and 0.25% nickel ammonium sulfate (Sigma-Aldrich, USA) for 10

min. All sections were mounted on gelatin-coated glass, air-dried overnight, dehydrated in graded ethanol, treated with TO-type biological transparentizing agent, and coverslipped using neutral quick drying glue. All sections were scanned using a digital whole-slide scanner and viewing software (NanoZoomer-XR, Japan).

Quantitative real-time polymerase chain reaction (qRT-PCR)

At 24 h after behavioral testing, brains were quickly removed from euthanized mice ($n=24$), followed by excision of the PFC and HPC. The specific primer sequences used for qRT-PCR are listed in Supplementary Table S1 (116 highly expressed genes in the brain were selected from the 207 glutamate-, GABA-, and inflammation-related candidate genes) and were designed according to reference sequences in PrimerBank or the NCBI database with Primer-BLAST. The primer sequences were synthesized by Qingke Biotechnology (China). Total RNA was extracted from the PFC and HPC using TRIzol reagent and reverse-transcribed into cDNA using a HiScript III All-In-One RT SuperMix Perfect for qPCR Kit (Cat# R333, Vazyme, China). After reverse transcription, qRT-PCR was carried out using the QuantStudio™ 1 Applied Biosystem Real-Time PCR System (Thermo Fisher Scientific, USA). The 20 μ L reaction system contained 10 μ L of PowerUp SYBR Green Master Mix (Cat. No. A25742; Applied Biosystems, USA), 0.5 μ L of each primer (forward and reverse), 4 μ L of cDNA template, and 5 μ L of nuclease-free deionized water. Two-step amplification was performed with denaturation at 95 °C for 3 min, followed by 40 cycles at 95 °C for 5 s and 60 °C for 30 s, and final elongation at 95 °C for 15 s, 60 °C for 1 min, and 95 °C for 15 s. The relative mRNA expression levels of selected genes were calculated with the 2^{– $\Delta\Delta$ Ct} method (Livak & Schmittgen, 2001), using hypoxanthine-guanine phosphoribosyltransferase (HPRT) as an internal reference. Each sample was tested in duplicate. Experimental group values were normalized to the control group.

Digital photomicrographs and data quantification

Photomicrographs were captured using a digital whole-slide scanner (NanoZoomer-XR, Japan). All digital images of brain sections were adjusted for cropping, brightness/contrast, and size using Adobe Photoshop CS6 (Adobe Systems, USA). The image files were processed in TIF format.

For quantitative analysis of the density of Iba1-immunoreactive (-ir) cell profiles in the PFC and HPC of mice, at least six sections from each mouse ($n=4–5$ mice per group) were selected for study. The density of Iba1-ir cell profiles was measured at 400× total magnification. Automatic cell counting was performed to analyze the sections using ImageJ software (NIH, USA, RRID:SCR_003070) based on previous studies (Choudhry, 2016; Grishagin, 2015). To avoid oversampling the same stained cells, the distance between adjacent brain sections was set to be greater than the diameter of the largest cells, as per previous study (Coggeshall and Lekan, 1996). Using ImageJ software, a random-offset grid (400 μ m×500 μ m) was applied to each image. Only grids in the regions of interest (PFC and HPC) were counted for each section. The density of Iba1-ir cell profiles was determined from the number of positive cell profiles per grid. Data from all grids in each region of each individual animal were pooled.

Statistical analysis

Statistical analysis was performed using SPSS v25 (SPSS,

USA, <http://www-01.ibm.com/software/uk/analytics/spss/>, RRID: SCR_002865). All results are expressed as mean±standard error of the mean (SEM). For normally distributed data, group differences in behavioral measures were tested using one-way or two-way analysis of variance (ANOVA), followed by Bonferroni's *post hoc* test. For non-normally distributed data, group differences were compared using the Kruskal-Wallis *H* test with Bonferroni correction in pairwise analyses. Multivariate analysis of covariance, followed by Bonferroni's *post hoc* test was performed for gene expression. Spearman correlation analysis (*r* and *P*-values) between gene expression and behavioral changes or between two genes was calculated using SPSS v25. Relationships between microglial density and behavioral changes were assessed using Pearson correlation analysis. Hierarchical clustering analysis and heatmap generation were performed using the pheatmap package in R. Effect size was calculated using Cohen's *d*. Significance was set at *P*<0.05. Data were plotted using GraphPad Prism (GraphPad Software, USA, RRID: SCR_002798).

RESULTS

Microglial depletion in PFC and HPC with administration of PLX3397 in drinking water

To determine the time course of the effects of the CSF1R/c-Kit kinase inhibitor (PLX3397) on microglia number in adult mouse brains, we treated 8-week-old mice with PLX3397 in drinking water (1 mg/mL) for 0, 7, 14, or 21 days (Figure 1A). Representative microphotographs of Iba1 immunostaining revealed a rapid time-dependent reduction in microglial density in the PFC and HPC (Figure 1B–G), with a 60% and 50% reduction, respectively, 7 days after PLX3397 administration (Figure 1D; $F(3, 16)=33.021$, $P<0.001$; Figure 1G; $F(3, 16)=27.196$, $P<0.001$) and a 95% and 93% reduction, respectively, 21 days after PLX3397 administration (Figure 1D, G).

PLX3397-mediated microglia depletion mitigates MK-801-induced hyperactivity and schizophrenia-like behaviors in mice

Administration of a low concentration of MK-801 increased the total distance moved in the OFT, whereas a high concentration decreased the total distance moved (Figure 2A; $F(4, 60)=15.20$, $P<0.001$). As shown in the line graph, single administration of MK-801 (0.1 mg/kg) regulated the total distance moved by mice in a time-dependent manner (Figure 2B). Behavioral tests were performed 30 min after single administration of MK-801 (Figure 2C). PLX3397 administration led to >70% depletion of microglia in the PFC and HPC and affected microglial morphology within 14 days (Figure 2D–F; Supplementary Figure S1). Quantitative analysis revealed that MK-801 significantly increased the total distance moved in the OFT (Figure 2G, H; PLX3397: ($F(1, 44)=0.016$, $P>0.05$), MK-801: ($F(1, 44)=32.766$, $P<0.001$), PLX3397×MK-801 interaction: ($F(1, 44)=0.426$, $P>0.05$)), time spent in the central area (Figure 2I; PLX3397: ($F(1, 44)=6.253$, $P<0.05$), MK-801: ($F(1, 44)=24.061$, $P<0.001$), PLX3397×MK-801 interaction: ($F(1, 44)=6.209$, $P<0.05$)), frequency of entries into the central area (Figure 2J; PLX3397: ($F(1, 44)=6.794$, $P<0.05$), MK-801: ($F(1, 44)=38.996$, $P<0.001$), PLX3397×MK-801 interaction: ($F(1, 44)=6.239$, $P<0.05$)), time spent in the open arms (Figure 2K–L; PLX3397:

($F(1, 44)=1.994$, $P>0.05$), MK-801: ($F(1, 44)=27.527$, $P<0.001$), PLX3397×MK-801 interaction: ($F(1, 44)=6.089$, $P<0.05$)), frequency of entries into the open arms (Figure 2M; Kruskal-Wallis *H* test, $H=27.108$, $P<0.001$), and total distance moved in the EPM (Figure 2N; PLX3397: ($F(1, 44)=3.152$, $P>0.05$), MK-801: ($F(1, 44)=45.176$, $P<0.001$), PLX3397×MK-801 interaction: ($F(1, 44)=10.761$, $P<0.01$)), while pretreatment with PLX3397 for 14 days significantly reversed these changes (Figure 2I–N). In addition, administration of PLX3397 in drinking water reversed the total duration of immobility (velocity<1.75 cm/s) induced by a single injection of MK-801 (Figure 2O; PLX3397: ($F(1, 44)=1.088$, $P>0.05$), MK-801: ($F(1, 44)=30.544$, $P<0.001$), PLX3397×MK-801 interaction: ($F(1, 44)=9.138$, $P<0.01$)). In the PPI test, depletion of microglia after PLX3397 administration significantly increased the MK-801-induced decrease in the percentage of PPI at 74 and 78 dB but not at 86 dB (Figure 2P; $P<0.05$). Elimination of microglia reversed the MK-801-induced increase in startle amplitude (Figure 2Q; $F(3, 40)=3.552$, $P<0.05$).

Repopulation of microglia does not affect hyperactivity induced by MK-801

To determine the time course of the effects of PLX3397 withdrawal on microglia number in the PFC and HPC, we treated 8-week-old mice with PLX3397 in drinking water (1 mg/mL) for 14 days, followed by PLX3397 withdrawal for 1, 3, 7, 14, or 21 days (Supplementary Figure S2A). Iba1 staining of the PFC and HPC showed that microglial density increased markedly after 7 days compared to 1 day of PLX3397 withdrawal (Supplementary Figure S2B–G; PFC: $F(5, 20)=34.189$, $P<0.001$; HPC: $F(5, 20)=11.794$, $P<0.001$). A similar number of microglia in the PFC and HPC was observed at 7, 14, and 21 days after PLX3397 withdrawal (Supplementary Figure S2D, G). Adult mice were treated with PLX3397 in drinking water for 14 days to eliminate microglia in the brain and then with drinking water for 21 days to allow microglial repopulation (Figure 3A). In the OFT and EPM, mice treated with MK-801 showed a significant increase in total distance moved (Figure 3B, C; PLX3397 withdrawal: ($F(1, 36)=0.971$, $P>0.05$), MK-801: ($F(1, 36)=23.125$, $P<0.001$), PLX3397 withdrawal×MK-801 interaction: ($F(1, 36)=1.450$, $P>0.05$)), time spent in the central area (Figure 3D; PLX3397 withdrawal: ($F(1, 36)=0.086$, $P>0.05$), MK-801: ($F(1, 36)=11.507$, $P<0.01$), PLX3397 withdrawal×MK-801 interaction: ($F(1, 36)=0.498$, $P>0.05$)), frequency of entries into the central area (Figure 3E; Kruskal-Wallis *H* test, $H=15.008$, $P<0.01$), time spent in the open arms (Figure 3F; PLX3397 withdrawal: ($F(1, 36)=0.149$, $P>0.05$), MK-801: ($F(1, 36)=15.106$, $P<0.001$), PLX3397 withdrawal×MK-801 interaction: ($F(1, 36)=0.005$, $P>0.05$)), and frequency of entries into the open arms (Figure 3G; Kruskal-Wallis *H* test, $H=22.553$, $P<0.01$) compared to the control group, whereas no differences in behavior were observed in the microglia-repopulated mice (PLX3397-repopulation, PLX-repo) compared to the MK-801-treated mice. Furthermore, no significant differences were found in microglial density among the four groups (Figure 3H–J).

Minocycline-mediated inhibition of microglial activation does not affect hyperactivity induced by MK-801

To investigate the effects of minocycline, an inhibitor of

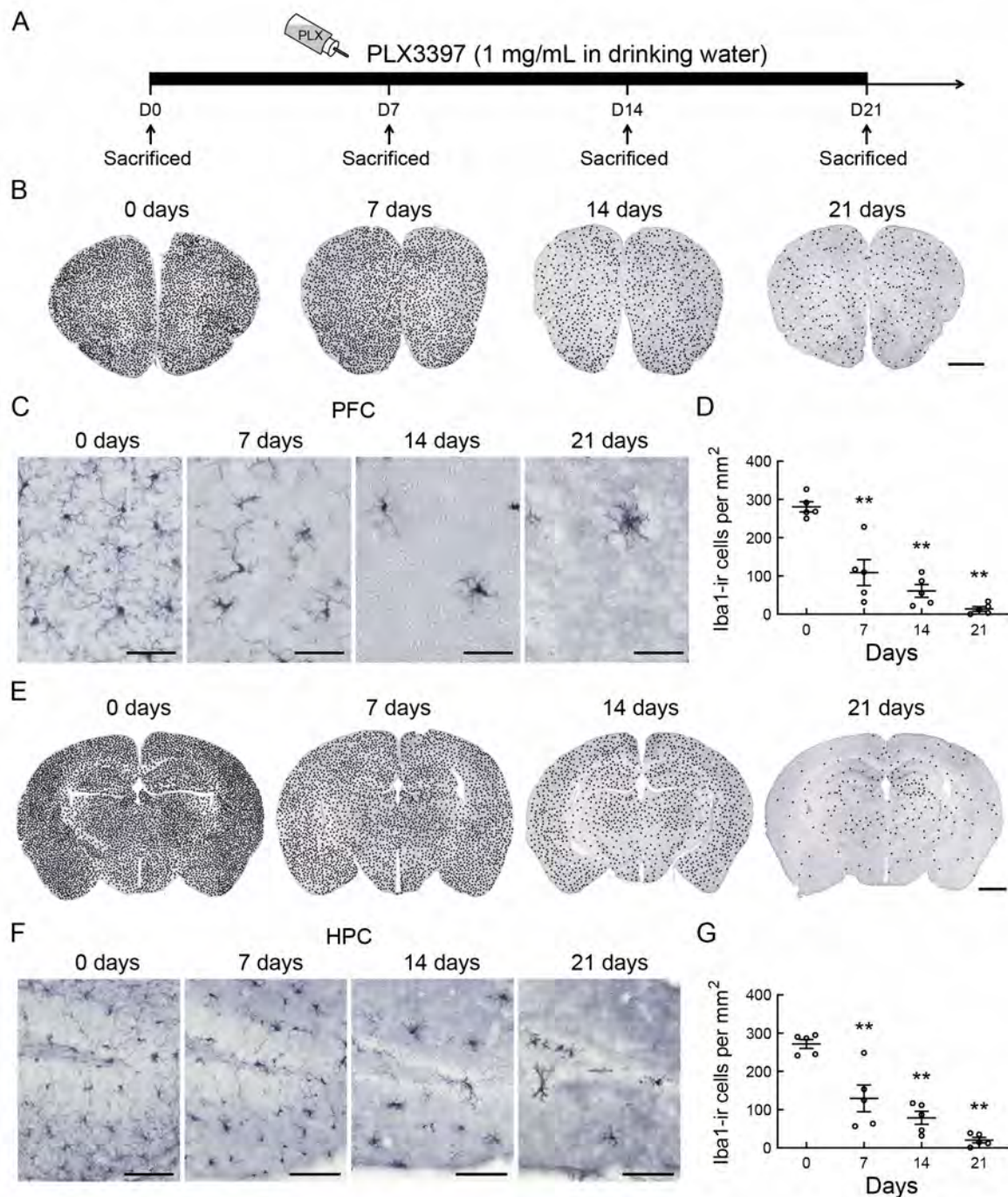


Figure 1 CSF1R inhibition by pexidartinib (PLX3397) rapidly depletes microglia from the adult mouse brain

A: Schematic of experimental design. B–G: Representative images show microglial changes (Iba1 immunoreactivity, microglial marker) in PFC (B, C) and HPC (E, F) after PLX3397 (1 mg/mL in drinking water) administration for 0, 7, 14, or 21 days. Quantification of microglial density in PFC (D) and HPC (G) after PLX3397 administration for 0, 7, 14, or 21 days ($n=5$ for each time point). Statistical analyses were performed via one-way ANOVA with Bonferroni's *post hoc* test. **: $P<0.01$ compared to 0 days. Density of black dots represents relative density of Iba1-ir cells in the brain. Each dot represents approximately two Iba1-ir cells. Scale bars: 1 000 μm in B, E; 50 μm in C; 100 μm in F.

microglial activation, on MK-801-induced hyperactivity, we injected (i.p.) minocycline (50 mg/kg) and MK-801 (0.1 mg/kg) into mice (Supplementary Figure S3A). MK-801 administration significantly increased the total distance moved (Supplementary Figure S3B, C, minocycline: ($F(1, 44)=1.667$, $P>0.05$), MK-801: ($F(1, 44)=57.681$, $P<0.001$), minocycline \times MK-801 interaction: ($F(1, 44)=0.405$, $P>0.05$)), time spent in the central area (Supplementary Figure S3D, minocycline: ($F(1, 44)=0.001$, $P>0.05$), MK-801: ($F(1,$

$44)=18.212$, $P<0.001$), minocycline \times MK-801 interaction: ($F(1, 44)=0.501$, $P>0.05$)), frequency of entries into the central area (Supplementary Figure S3E, Kruskal-Wallis H test, $H=27.991$, $P<0.001$), time spent in the open arms (Supplementary Figure S3F, minocycline: ($F(1, 44)=0.692$, $P>0.05$), MK-801: ($F(1, 44)=17.974$, $P<0.001$), minocycline \times MK-801 interaction: ($F(1, 44)=2.358$, $P>0.05$)), and frequency of entries into the open arms (Supplementary Figure S3G, Kruskal-Wallis H test, $H=20.754$, $P<0.001$) compared to the control group, with these

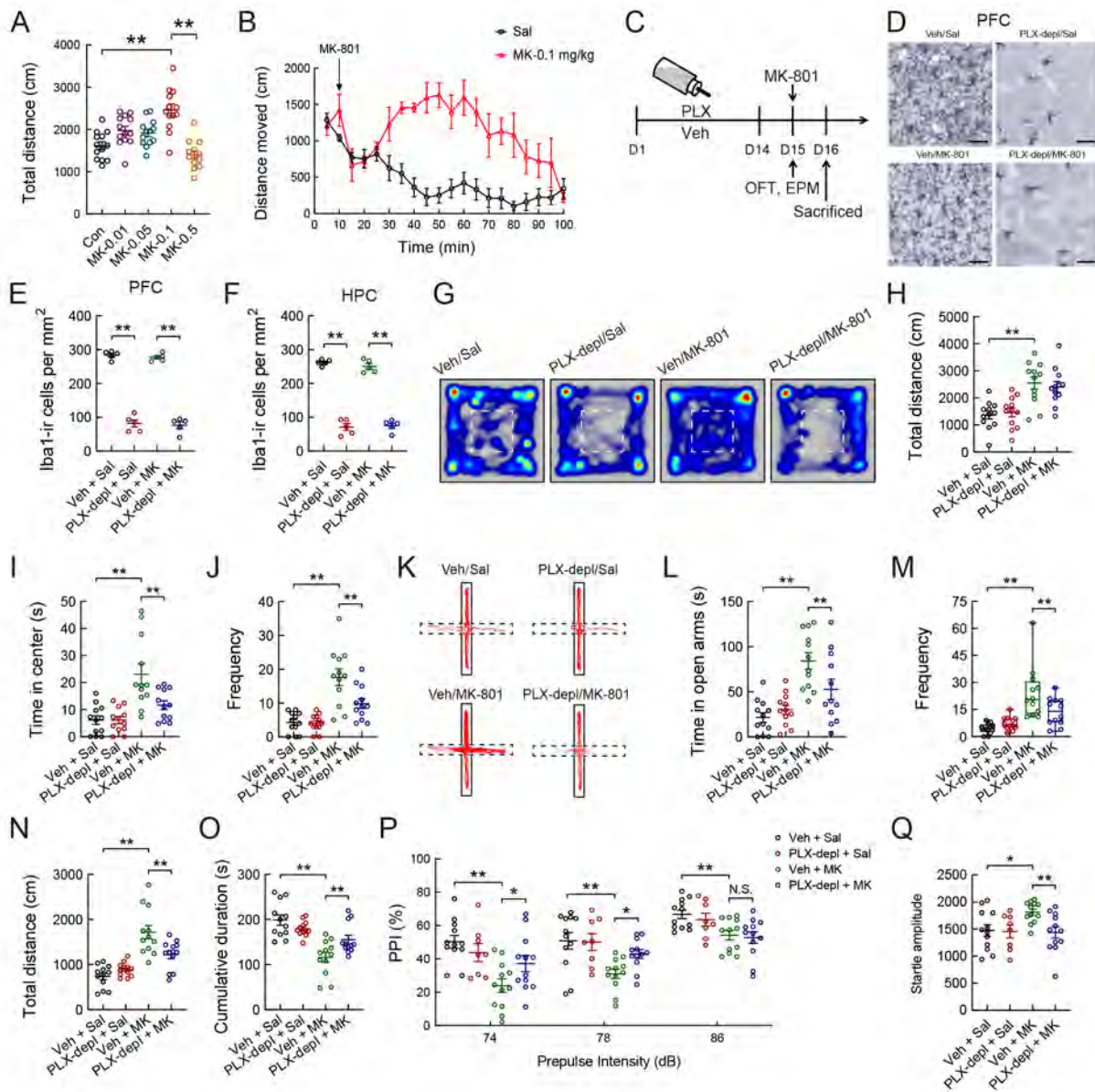


Figure 2 Depletion of microglia by CSF1R inhibitor PLX3397 mitigates anxiety-like and schizophrenia-like behaviors induced by NMDA receptor antagonist MK-801 (dizocilpine) in mice

A: Total distance moved in open-field box 30 min after single injection of MK-801 (0, 0.01, 0.05, 0.1, or 0.5 mg/kg). B: Total distance moved in open-field box before and after single injection of MK-801 (0.1 mg/kg) or saline. C: Schematic of experimental design. D–F: Photomicrographs of Iba1-ir staining of PFC (D) after single injection of MK-801 or saline with PLX3397 (PLX) or vehicle pretreatment, respectively, for 14 days. Quantification of microglial density in PFC (E) and HPC (F) after PLX and/or MK-801 administration ($n=5$ for each group). G: Heatmaps showing cumulative duration spent by each group within the compartment during OFT. Dashed lines represent central areas. H: Total distance moved by each group in the box during 5 min OFT. I: Time spent by each group in the central area. J: Comparison of frequency of entries into central area of open-field among four groups after PLX and/or MK-801 administration. K: Representative tracks of PLX- and/or MK-801-treated mice during 5 min EPM test. Dashed lines represent open arms. L: Time spent in open arms during 5 min EPM test among four groups. M: Frequency of entries into open arms. Statistical analyses were performed using Kruskal-Wallis H test with Bonferroni's *post hoc* test. **: $P < 0.01$. N: Total distance moved by each group in the maze. O: Total duration of immobility (velocity < 1.75 cm/s) of PLX- and/or MK-801-treated mice in the maze during 5 min EPM test. P, Q: Depletion of microglia with PLX3397 attenuates MK-801-induced deficits in percentage PPI (% PPI) of acoustic startle reflex (P) and startle amplitude (Q). Statistical analyses were performed via two-way ANOVA or Kruskal-Wallis H test with Bonferroni's *post hoc* test ($n=12$ /group). N.S.: Not significant; * $P < 0.05$; ** $P < 0.01$. MK, MK-801; PLX-depl, PLX3397 depletion; Sal, saline; Veh, vehicle. Scale bars: 50 μ m in A; 100 μ m in C.

behavioral changes not reversed by minocycline pretreatment (Supplementary Figure S3C–G).

Association of hyperactivity with microglial density in PFC and HPC

Based on the variability in microglial density in the brains of

mice pretreated with PLX3397 for 0, 4, 8, 10, or 12 days, we investigated the correlation between microglia and behaviors in the OFT and EPM. In the OFT, PLX3397-controlled Iba1-ir cell density in the PFC and HPC was positively correlated with total distance moved (Figure 4A, $r=0.599$, $P < 0.01$; Figure 4I, $r=0.672$, $P < 0.01$) and negatively correlated with total duration

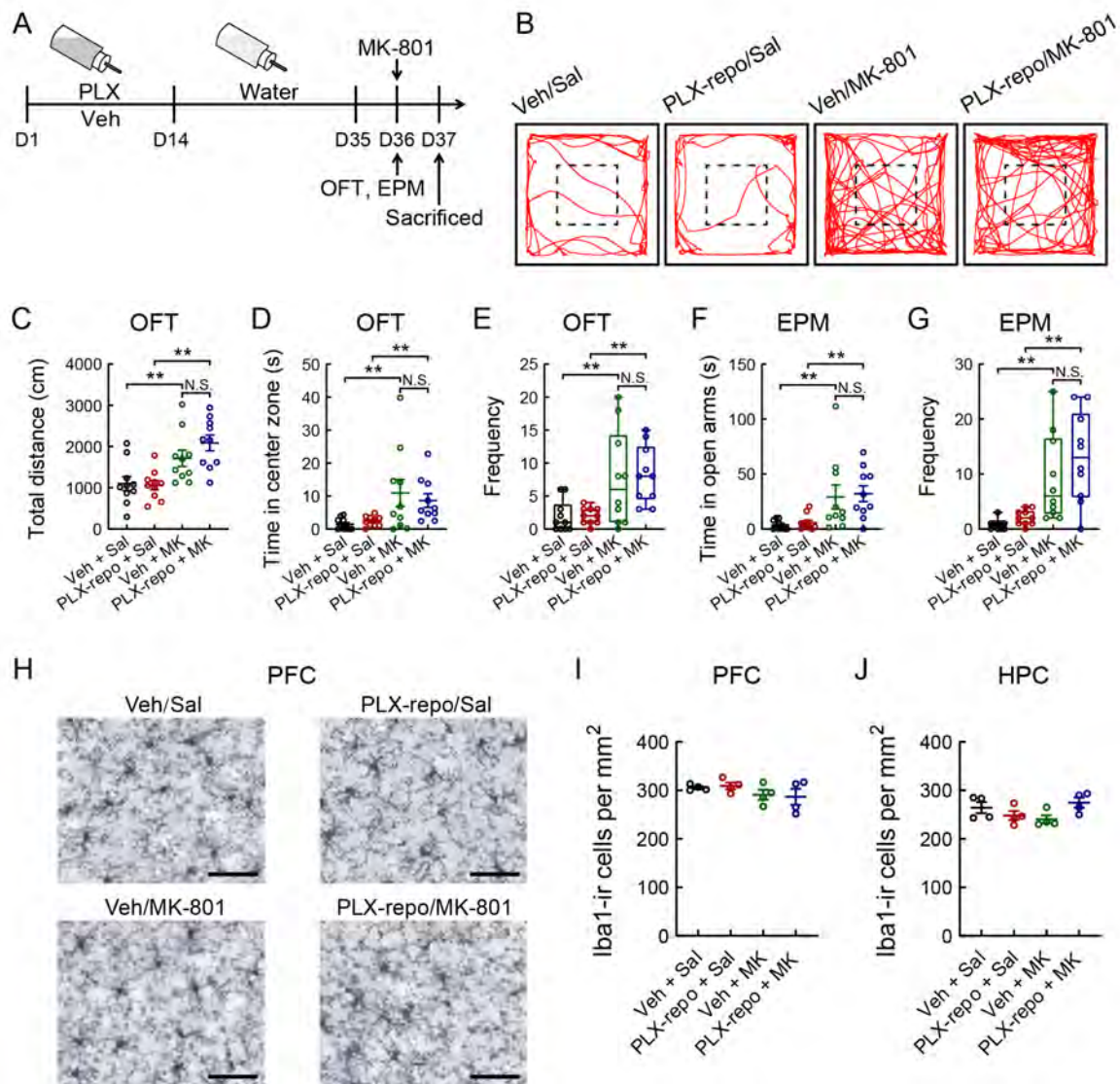


Figure 3 Repopulation of microglia after removal of CSF1R inhibitor PLX3397 has no effect on anxiolytic-like behaviors induced by NMDA receptor antagonist MK-801 in mice

A: Schematic of experimental design. B: Example tracks of PLX- and/or MK-801-treated mice during 5 min OFT. Dashed lines represent central areas. C: Total distance moved by each group in the box during 5 min OFT. D: Time spent by each group in central area. E: Comparison of frequency of entries into central area of open-field among four groups after PLX3397 (PLX) and/or MK-801 administration. F: Time spent in open arms during 5 min EPM test among four groups. G: Frequency of entry into open arms by each group after PLX and/or MK-801 administration. H: Photomicrographs of Iba1-ir staining in PFC after single injection of MK-801 or saline with PLX3397 (1 mg/mL in drinking water) or vehicle administration for 14 days, followed by PLX3397 or vehicle withdrawal for 21 days. I, J: Quantification of microglial density in PFC (I) and HPC (J) after PLX and/or MK-801 administration ($n=4$ /group). Statistical analyses were performed via two-way ANOVA or Kruskal-Wallis H test (E, G) with Bonferroni's *post hoc* test ($n=10$ /group). N.S.: Not significant; **: $P<0.01$. MK, MK-801; PLX-repo, PLX3397-repopulation; Sal, saline; Veh, vehicle. Scale bars: 50 μ m in H.

of immobility (Figure 4B, $r=-0.570$, $P<0.05$; Figure 4J, $r=-0.681$, $P<0.01$). However, no correlation was found between microglial density and duration or frequency (Figure 4C, D; Figure 4K–L). In the EPM test, a similar correlation between microglial density in the PFC and behavior was observed (Figure 4E–H). Additionally, Iba1-ir cell density in the HPC was positively correlated with total distance moved (Figure 4M, $r=0.656$, $P<0.01$), time spent in the open arms (Figure 4O, $r=0.481$, $P<0.05$), and frequency of entries into the open arms (Figure 4P, $r=0.579$, $P<0.01$), but negatively correlated with total duration of immobility (Figure 4N, $r=-0.691$, $P<0.01$).

Effects of PLX3397 and MK-801 administration on glutamate- and GABA-related gene expression profiles in PFC and HPC

To test the effects of PLX3397 and MK-801 administration on glutamate- and GABA-related gene expression profiles in the brain, we injected (i.p.) PLX3397 (50 mg/kg) and MK-801 (0.1 mg/kg) into mice (Figure 5A). Based on behavioral analysis, the MK-801-treated mice showed a significant increase in total distance moved and frequency of entries into the central area and a significant decrease in total duration of immobility compared to the control group, whereas PLX3397 treatment reversed these effects in the MK-801-treated mice (Figure 5B, $F(3, 20)=11.691$, $P<0.001$; Figure 5C, $F(3,$

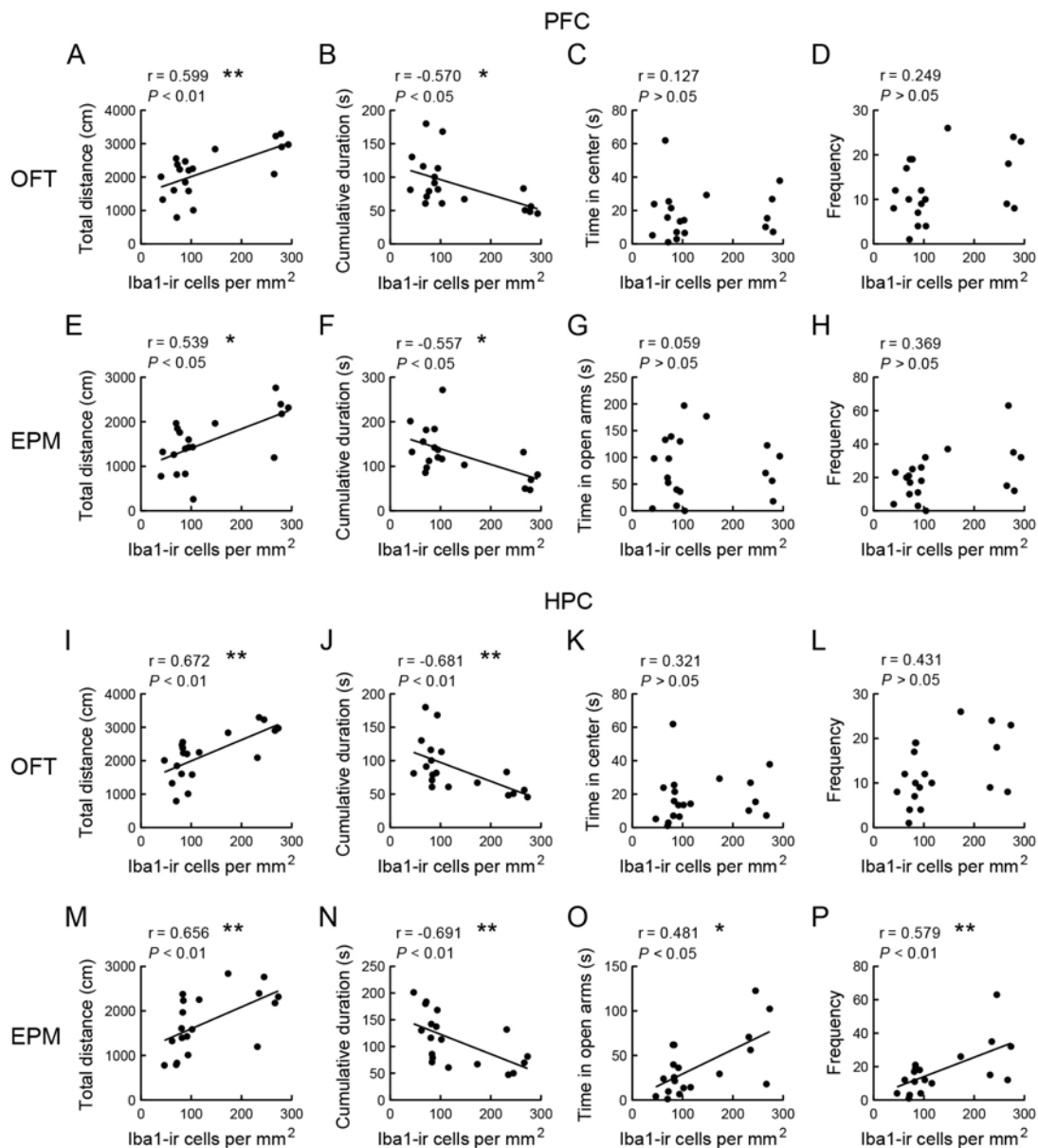


Figure 4 Correlation between microglial density in the brain and anxiolytic-like behaviors in mice

A–H: Correlation between Iba1-ir cells in PFC and behaviors in OFT (A: Total distance; B: Cumulative duration of immobility; C: Center duration; D: Frequency of entries into central area) and EPM test (E: Total distance; F: Cumulative duration of immobility; G: Time spent in open arms; H: Frequency of entries into open arms). I–P: Correlation between Iba1-ir cells in HPC and behaviors in OFT and EPM. Correlation coefficients (r) and P -values were determined using Pearson correlation analysis ($n=19$). *: $P < 0.05$; **: $P < 0.01$.

20)=8.156, $P < 0.001$; Figure 5D, $P < 0.01$). qRT-PCR analysis was used to determine glutamate- and GABA-related gene expression in different groups (Figure 5E–K; Supplementary Figure S4). As shown in the graphs, the expression levels of six genes in the PFC and HPC were significantly affected by PLX3397 exposure (Figure 5F–K). In the PFC, 20 of the 38 tested target genes were significantly up-regulated in the PLX3397-treated mice, while only five genes were significantly up-regulated in the MK-801-treated mice (Figure 5E–I). In the HPC, nine of the 36 tested target genes were significantly up-regulated and one was significantly down-regulated in the PLX3397-treated mice, whereas four genes were significantly up-regulated in the MK-801-treated mice (Figure 5E, J, K). Furthermore, in the MK-801-treated mice, PLX3397 administration significantly up-regulated the mRNA expression levels of six genes (*Gria2*, *Gria3*, *Gad1*, *Slc1a2*, *Grm1*, and

Grin2a) in the PFC but only significantly up-regulated the mRNA expression of *VIAAT* and down-regulated the mRNA expression of *Grm2* in the HPC (Figure 5E–K). We also performed correlation analysis of these differentially expressed glutamate- and GABA-related genes in the PFC and HPC with behaviors (center time and frequency of entries into the central area in the OFT). However, no correlations were observed between behaviors and gene expression in the PFC and HPC (Figure 5L). A correlation matrix was constructed to show the relationships among the differentially expressed glutamate- and GABA-related genes in the brain (Figure 5M).

Effects of PLX3397 and MK-801 administration on inflammation-related gene expression profiles in the brain

To verify the effects of PLX3397 and MK-801 treatment on inflammation-related gene expression profiles in the brain, we

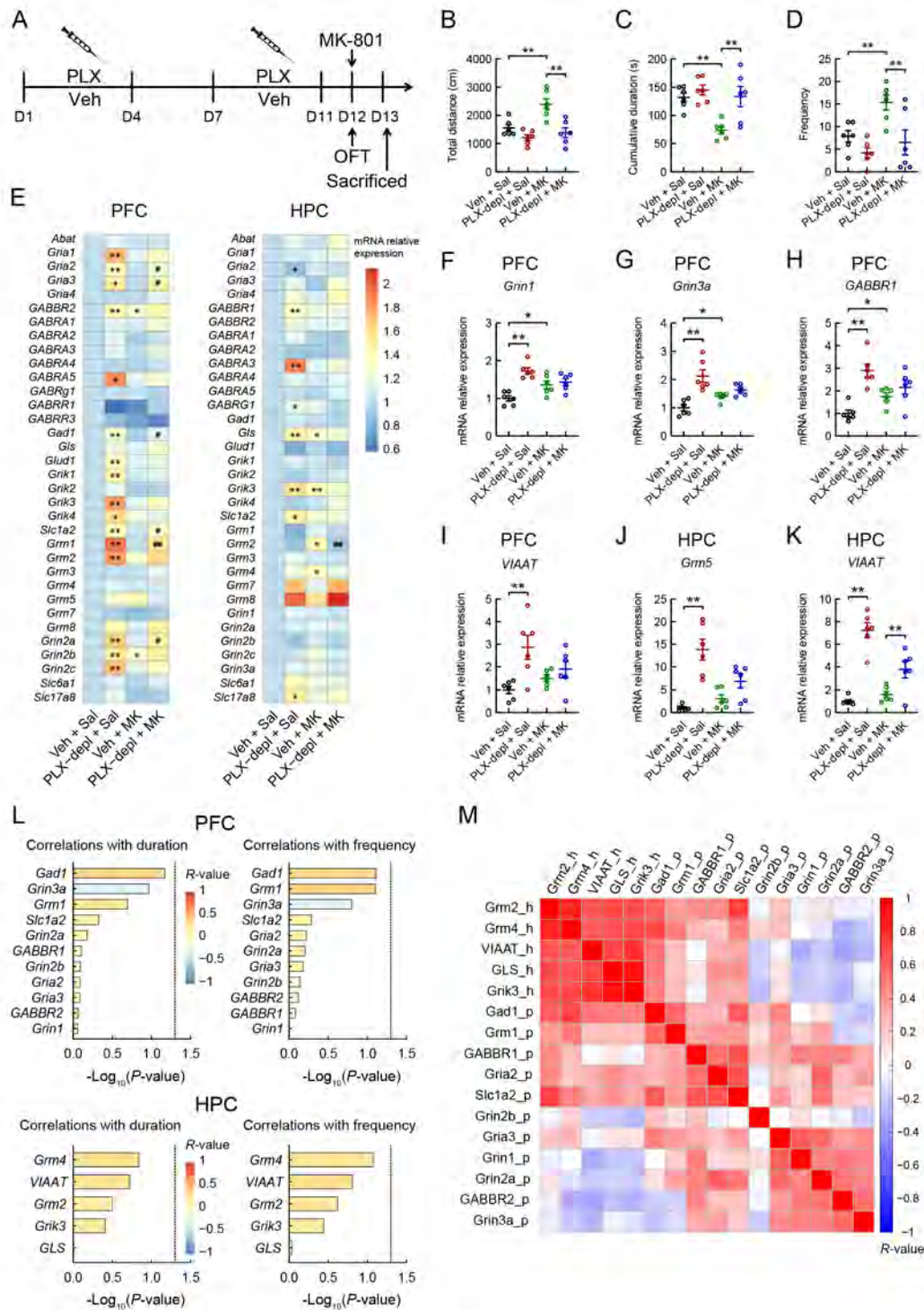


Figure 5 Effects of PLX3397 and MK-801 administration on hyperactivity and levels of glutamate- and GABA-related gene expression in mouse brains

A: Schematic of experimental design. B–D: Effects of PLX3397 (50 mg/kg) and MK-801 (0.1 mg/kg) administration on total distance moved, cumulative duration of immobility, and frequency of entries into central area during OFT. E: Heatmaps showing glutamate- and GABA-related gene expression values in different groups. * compared to Veh+Sal; † $P < 0.05$; †† $P < 0.01$; # compared to Veh+MK; #† $P < 0.05$; #†† $P < 0.01$. F–K: Quantitative analysis showing effects of PLX3397 pretreatment on MK-induced gene expression in PFC and HPC. Statistical analyses were performed via two-way ANOVA with Bonferroni's *post hoc* test ($n=6$ /group). † $P < 0.05$; †† $P < 0.01$. L: Correlations of differentially expressed glutamate- and GABA-related gene expression levels in PFC and HPC with behaviors (center duration and frequency of entries into central area in OFT). Color scale indicates r -value. P -value was calculated using Spearman correlation test with a significance threshold of $P \leq 0.05$. X-axis is $-\log_{10}$ -transformed P -values (indicated by dotted line of $-\log_{10}(P\text{-value})=1.3$). M: Heatmap showing pairwise correlations among differentially expressed glutamate- and GABA-related gene expression levels in PFC (represented by the suffix “_p”) and HPC (represented by the suffix “_h”). Color corresponds to value of Spearman correlation coefficient, with red and blue indicating positive and negative correlations, respectively. MK, MK-801; PLX-depl, PLX3397 depletion; Sal, saline; Veh, vehicle.

selected 80 inflammation-related genes with high expression in the brain. The qRT-PCR data showed inflammation-related gene expression profiles in the PFC and HPC in the four groups (Figure 6; all candidate inflammation-related gene expression profiles, including astrocyte functional genes, chemokines, colony stimulating factors, complements, complement factors, cytokines, microglial functional genes, mitochondrial functional genes, Toll-like receptors, transmembrane proteins, and phagocytosis, are shown in Supplementary Figure S5). The graphs show the expression levels of 25 genes in the PFC and 25 genes in the HPC that were the most significantly affected by PLX3397 exposure (Figure 6A2-A26, B2-B26). In the PFC, 34 of the 80 tested target genes were significantly up-regulated and 11 were significantly down-regulated in the PLX3397-treated mice, but only three genes (*IKBKG*, *CX3CR1*, and *TMEM119*) were significantly up-regulated in the MK-801-treated mice (Figure 6A1-A26). In the HPC, 35 of the 78 tested target genes were significantly up-regulated and 11 were significantly down-regulated in the PLX3397-treated mice, but only eight genes were significantly up-regulated in the MK-801-treated mice (Figure 6B1-B26). Moreover, PLX3397 exposure in the MK-801-treated mice significantly up-regulated the mRNA expression levels of 23 genes (*ATP5A1*, *CFB*, *CXCL12*, *IL-33*, *TMEM176a*, *TMEM176b*, *TMEM45a*, *TMEM59*, *CCL2*, *CCL5*, *CXCL5*, *CXCL10*, *CXCL16*, *TLR2*, *TLR3*, *SERPING*, *TMEM16a*, *CSF1*, *TNFA*, *IL-1b*, *IL-4*, *C2*, and *GFAP*) and down-regulated the mRNA expression levels of 12 genes (*C1qb*, *CFH*, *CSF3R*, *CSF1R*, *CX3CR1*, *CD206*, *CD11b*, *CD68*, *CD163*, *F4/80*, *TREM2*, and *TMEM119*) in the PFC (Figure 6A1-A26), but significantly up-regulated the mRNA expression levels of 18 genes and down-regulated the mRNA expression levels of 16 genes in the HPC (Figure 6B1-B26).

Association of inflammation-related gene expression levels in the PFC and HPC with MK-801-induced behaviors

We performed a correlation analysis to determine the associations between behavioral performance and levels of differentially expressed inflammation-related genes (Figure 6C, D). Significant positive correlations were found between center time in the OFT and *CD206*, *F4/80*, and *TMEM119* expression, as well as between center frequency and *TMEM176a* and *TMEM119* expression in the PFC (Figure 6C; Supplementary Figure S6). In the HPC, significant positive correlations were found between center time and *NLRP3*, *TMEM119*, *TMEM176a*, *F4/80*, and *CD163* expression, as well as between center frequency and mRNA expression levels of *NLRP3* and *CD163* (Figure 6D; Supplementary Figure S6). Correlation matrices illustrated the relationships among the differentially expressed inflammation-related genes in the PFC and HPC (Supplementary Figure S7). Hierarchical clustering identified distinct sets of differentially expressed inflammation-related genes with strong correlations, including 11 genes in the PFC (*CD68*, *CD163*, *C1qb*, *CD206*, *TMEM119*, *CSF3R*, *CX3CR1*, *TREM2*, *CD11b*, *CSF1R*, and *F4/80*) and 14 genes in the HPC (*CX3CR1*, *CD68*, *NLRP3*, *Iba1*, *TLR9*, *CD206*, *TMEM119*, *F4/80*, *CD11b*, *CSF1R*, *CSF3R*, *TREM2*, *CD163*, and *IRF5*) (Supplementary Figure S7A-B). The strongest correlations were observed between *CSF1R* and *F4/80* in the PFC (correlation coefficient 0.993; $-\log_{10}(P\text{-value})=21.301$) and

between *CSF1R* and *CD11b* in the HPC (correlation coefficient 0.991; $-\log_{10}(P\text{-value})=19.953$) (Supplementary Figure S7C, D).

DISCUSSION

Our results showed rapid elimination and repopulation of microglia in the PFC and HPC of mice following administration and withdrawal of the dual CSF1R/c-Kit kinase inhibitor PLX3397 in drinking water. Drinking water containing PLX3397 is cost effective and easily prepared in the laboratory compared to animal chow containing PLX3397, which is expensive and needs to be commercially mixed. Administration of PLX3397 in mice to deplete microglia prevented hyperactivity and schizophrenia-like behaviors induced by MK-801. However, both repopulation of microglia after withdrawal of PLX3397 and inhibition of microglia activation by minocycline had no effects on hyperactivity induced by MK-801. Additionally, *Iba1-ir* cell density in the PFC and HPC was correlated with behavioral changes in the OFT and EPM. We also observed common and distinct glutamate-, GABA-, and inflammation-related gene expression patterns in the PFC and HPC of PLX3397- and/or MK-801-treated mice. Results showed no significant correlations between glutamate- and GABA-related gene expression changes and center time or frequency in the PLX3397- and MK-801-treated mice. However, significant correlations were found between inflammation-related gene expression changes in the brain and center time and frequency in the OFT.

Mice treated with PLX3397 and PLX5622 using standard chow diet, oral gavage, intracerebroventricular injection, or i.p. injection show depleted microglia/macrophages in the brain (Chen et al., 2022; Elmore et al., 2014; Ma et al., 2020; Najafi et al., 2018; Zhang et al., 2020). Similarly, in our study, mice treated with PLX3397-containing drinking water showed a rapid elimination of microglia in the PFC and HPC. After 7 days of PLX3397 withdrawal, newborn microglia rapidly repopulated the PFC and HPC. Our data showed that elimination of microglia in the brain prevented hyperactivity in the center zone of the OFT and open arms of the EPM, as well as schizophrenia-like behavior induced by MK-801 in mice. Consistent with our findings, depletion of microglia by PLX3397 can block the antidepressant effects of the NMDAR antagonist ketamine in mice susceptible to chronic social defeat stress (Yao et al., 2022a). Other studies have reported an increase in miniature excitatory postsynaptic current (mEPSC) frequency and decrease in the α -amino-3-hydroxy-5-methyl-4-isoxazolepropionic acid (AMPA)/N-methyl-D-aspartate (NMDA) current ratio in the visual cortex of PLX3397-treated developing mice (Ma et al., 2020). Recent evidence has also indicated that microglial depletion with PLX3397 is associated with a decrease in total and NMDAR-mediated synaptic transmission in the brain, specifically in young rodents (Yegla et al., 2021). Our study showed that *Grin1* and *Grin3a* gene expression levels increased in the brains of PLX3397-treated mice. Blocking NMDAR-mediated synaptic transmission by MK-801 also increased the expression of *Grin1* and *Grin3a*. Our findings indicate that *Grin1* and *Grin3a* may play a key role in NMDAR-mediated synaptic transmission. These results in the cortex of immature and adult mice are consistent with other studies examining gene expression (Smith et al., 2020). These findings suggest that PLX3397 influences microglia-mediated synaptic remodeling and pruning by modulating gene expression in the

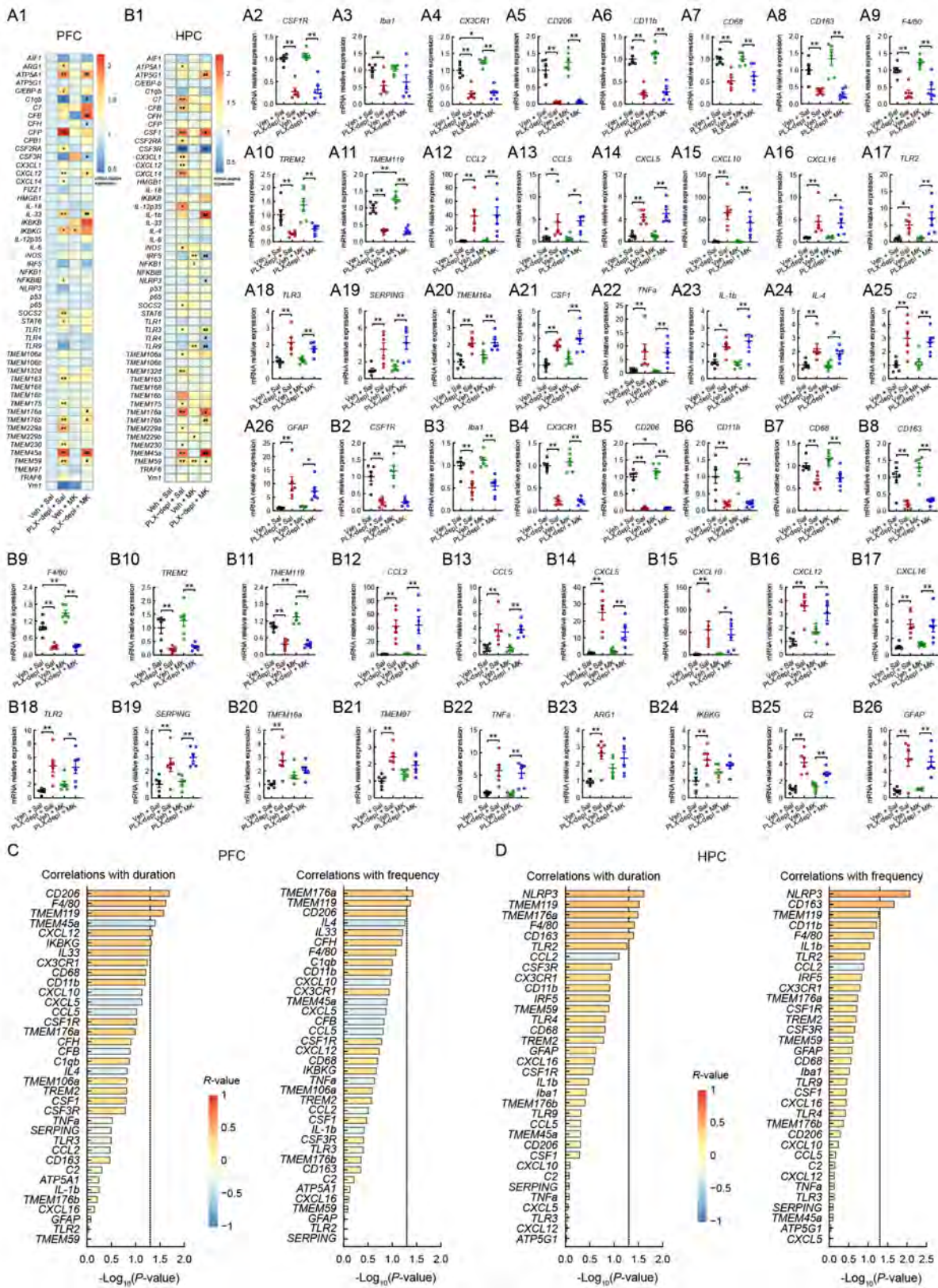


Figure 6 Effects of PLX3397 and MK-801 treatment on inflammation-related gene expression profiles in PFC and HPC of mice
 A1, B1: Heatmap showing relative expression of inflammation-related genes in PFC and HPC in different groups. * compared to Veh+Sal; **: $P < 0.05$; ***: $P < 0.01$; # compared to Veh+MK; #: $P < 0.05$; ###: $P < 0.01$. A2-A26, B2-B26: Quantitative analysis showing effects of PLX3397 pretreatment on MK-801-induced gene expression profiles in PFC (A2-A26) and HPC (B2-B26). Statistical analyses were performed via two-way ANOVA with Bonferroni's *post hoc* test ($n=6$ /group). *: $P < 0.05$; **: $P < 0.01$. C, D: Correlations between differentially expressed inflammation-related gene expression levels in PFC and HPC and behaviors (center duration and frequency of entries into central area in OFT). Color scale indicates r -value. P -value was calculated using Spearman correlation test with a significance threshold of $P \leq 0.05$ ($n=24$). X-axis is $-\log_{10}$ -transformed P -values (indicated by dotted line of $-\log_{10}(P\text{-value})=1.3$). MK, MK-801; PLX-depl, PLX3397 depletion; Sal, saline; Veh, vehicle.

brain. An alternative possibility is that NMDAR function is decreased by PLX3397 exposure in adults, such that MK-801 administration is less effective.

Abnormalities in gut microbiota composition play an important role in psychiatric disorders (Hashimoto, 2022; Mcguinness et al., 2022; Yang et al., 2023; Yao et al., 2022b). Recent research has indicated that PLX5622 can produce long-lasting abnormalities in the gut microbiota of mice (Yang et al., 2022). Thus, abnormalities in gut microbiota after PLX3397 treatment may affect MK-801-induced behaviors.

As reported in previous research, MK-801-induced hyperlocomotion can be significantly attenuated by a single injection of minocycline (40 mg/kg, 30 min before MK-801 administration) in Std:ddy mice (Zhang et al., 2007), in contrast with our observations in chronic minocycline-treated C57BL/6 mice (minocycline administration stopped 12 h before behavioral testing). Minocycline has a short half-life (approximately 2 h) in rodents (Fagan et al., 2004) and its effects had likely disappeared before behavioral testing.

Importantly, we found that microglial density in the PFC and HPC was significantly correlated with behavioral changes in the PLX3397- and MK-801-treated mice. Collectively, these findings indicate that microglia play a major role in MK-801-induced hyperlocomotion. Microglia are resident macrophages located in the central nervous system (Ginhoux et al., 2010). Previous transcriptomic analyses have reported that PLX5622 administration to deplete microglia induces changes in the expression of inflammatory-, glutamate-, and GABA-related genes in the PFC of mice (Warden et al., 2020). In the present study, PLX3397 resulted in a larger number of genes with altered expression in the PFC than in the HPC. Moreover, glutamate- and GABA-related gene expression patterns induced by MK-801 differed between the PFC and HPC. However, further correlation analysis found no significant correlations between glutamate- and GABA-related gene expression and behavioral changes.

Interestingly, immune-related gene expression profiles in the PFC were similar to those in the HPC of PLX3397- and/or MK-801-treated mice. The CSF1R/c-Kit kinase inhibitor reduced the mRNA levels of microglial marker genes (*CSF1R*, *CX3CR1*, and *TREM2*) but increased the mRNA levels of metabotropic glutamate receptor genes (*Grm1* and *Grm2*), consistent with previous studies (Coleman et al., 2020; Elmore et al., 2014). Moreover, 10 common inflammation-related genes (*CD68*, *CD163*, *CD206*, *TMEM119*, *CSF3R*, *CX3CR1*, *TREM2*, *CD11b*, *CSF1R*, and *F4/80*) with strong correlations were identified in the PFC and HPC using hierarchical clustering analysis. Based on further correlation analysis, the most significant associations were detected between behavioral changes in the OFT and mRNA levels of *CD206*, *F4/80*, *TMEM119*, and *TMEM176a* in the PFC, and center time and frequency and *NLRP3*, *TMEM119*, *F4/80*, *CD163*, and *TMEM176a* expression in the HPC. Thus, the present study revealed that *CD163*, *CD206*, *F4/80*, *TMEM119*, *TMEM176a*, and *NLRP3* play important roles in NMDAR antagonist-mediated hyperactive behavior.

Our study has several limitations. First, further research using transgenic mouse models is needed to investigate the functions of the genes correlated with inflammation and their role in psychiatric disorders, including schizophrenia, depression, bipolar disorder, anxiety, suicidality, and Alzheimer's disease. Second, it remains unclear whether the inflammation-related effects observed were due to changes in

the PFC or HPC. Thus, more reliable data may be obtained by localized application of PLX3397 and MK-801. Third, further immunohistochemical and western blot analyses are necessary to confirm whether changes in behaviors and genes are associated with protein changes in the brain. In addition, electrophysiological experiments are needed to determine whether microglial depletion with PLX3397 is associated with a decrease in NMDAR-mediated synaptic transmission in the PFC and HPC. Finally, it is unclear which brain region may serve as an appropriate control that is both unaffected by PLX3397 and unrelated to the observed behaviors.

In summary, depletion of microglia with the CSF1R/c-Kit kinase inhibitor PLX3397 reverses hyperactivity induced by the NMDAR antagonist MK-801, which is associated with regulating inflammation-related genes in the PFC and HPC. Further investigations involving inflammation-related transgenic mice with microglial *NLRP3*, *CD163*, *CD206*, *F4/80*, *TMEM119*, and *TMEM176a* gene knockout will help to clarify the functional roles of these genes in psychiatric disorders, such as schizophrenia.

SUPPLEMENTARY DATA

Supplementary data to this article can be found online.

COMPETING INTERESTS

The authors declare that they have no competing interests.

AUTHORS' CONTRIBUTIONS

R.J.N. and Y.Y.W. were involved in experimental treatments of the animals, acquisition of data, interpretation of data, and writing of the manuscript. T.H.G. was involved in experimental treatments of the animals and tissue processing. Q.R.W. and Y.R.M. were involved in experimental treatments of the animals and histochemical analysis. J.X.W. and L.S.Z. were responsible for revising the manuscript. X.H.M. and T.L. were responsible for experimental design and revising the manuscript. All authors read and approved the final version of the manuscript.

ACKNOWLEDGMENTS

We would like to thank Juan Mei and Hong Bu (Institute of Clinical Pathology, West China Hospital of Sichuan University, Chengdu, 610041, China) for microscopic observations. We would also like to thank Ling-Hui Yang and Jing Wang (Laboratory of Anesthesia and Critical Care Medicine, Chengdu, 610041, China) for the PPI tests.

REFERENCES

- Bradford AM, Savage KM, Jones DNC, Kalinichev M. 2010. Validation and pharmacological characterisation of MK-801-induced locomotor hyperactivity in BALB/C mice as an assay for detection of novel antipsychotics. *Psychopharmacology*, **212**(2): 155–170.
- Chen PA, Wang HY, Sun CL, Chen ML, Chen YC. 2022. Neurobehavioral differences of valproate and risperidone on MK-801 inducing acute hyperlocomotion in mice. *Behavioural Neurology*, **2022**: 1048463.
- Choudhry P. 2016. High-throughput method for automated colony and cell counting by digital image analysis based on edge detection. *PLoS One*, **11**(2): e0148469.
- Coggeshall RE, Lekan HA. 1996. Methods for determining numbers of cells and synapses: a case for more uniform standards of review. *The Journal of Comparative Neurology*, **364**(1): 6–15.
- Coleman LG Jr, Zou J, Crews FT. 2020. Microglial depletion and repopulation in brain slice culture normalizes sensitized proinflammatory signaling. *Journal of Neuroinflammation*, **17**(1): 27.
- Elmore MRP, Najafi AR, Koike MA, Dagher NN, Spangenberg EE, Rice RA,

- et al. 2014. Colony-stimulating factor 1 receptor signaling is necessary for microglia viability, unmasking a microglia progenitor cell in the adult brain. *Neuron*, **82**(2): 380–397.
- Fagan SC, Edwards DJ, Borlongan CV, Xu L, Arora A, Feuerstein G, et al. 2004. Optimal delivery of minocycline to the brain: implication for human studies of acute neuroprotection. *Experimental Neurology*, **186**(2): 248–251.
- Ginhoux F, Greter M, Leboeuf M, Nandi S, See P, Gokhan S, et al. 2010. Fate mapping analysis reveals that adult microglia derive from primitive macrophages. *Science*, **330**(6005): 841–845.
- Gober R, Ardalan M, Shideh SMJ, Duque L, Garamszegi SP, Ascona M, et al. 2022. Microglia activation in postmortem brains with schizophrenia demonstrates distinct morphological changes between brain regions. *Brain Pathology*, **32**(1): e13003.
- Grishagin IV. 2015. Automatic cell counting with ImageJ. *Analytical Biochemistry*, **473**: 63–65.
- Hashimoto K. 2022. Gut-microbiota-brain axis by bile acids in depression. *Psychiatry and Clinical Neurosciences*, **76**(7): 281.
- Hwang Y, Kim J, Shin JY, Kim JI, Seo JS, Webster MJ, et al. 2013. Gene expression profiling by mRNA sequencing reveals increased expression of immune/inflammation-related genes in the hippocampus of individuals with schizophrenia. *Translational Psychiatry*, **3**(10): e321.
- Lanz TA, Reinhart V, Sheehan MJ, Rizzo SJS, Bove SE, James LC, et al. 2019. Postmortem transcriptional profiling reveals widespread increase in inflammation in schizophrenia: a comparison of prefrontal cortex, striatum, and hippocampus among matched tetrads of controls with subjects diagnosed with schizophrenia, bipolar or major depressive disorder. *Translational Psychiatry*, **9**(1): 151.
- Lei FY, Cui NW, Zhou CX, Chodosh J, Vavvas DG, Paschalis EI. 2020. CSF1R inhibition by a small-molecule inhibitor is not microglia specific; affecting hematopoiesis and the function of macrophages. *Proceedings of the National Academy of Sciences of the United States of America*, **117**(38): 23336–23338.
- Livak KJ & Schmittgen TD. 2001. Analysis of relative gene expression data using real-time quantitative PCR and the 2⁻(Delta Delta C(T)) Method. *Methods*, **25**(4): 402–408.
- Ma XK, Chen K, Cui YH, Huang GQ, Nehme A, Zhang L, et al. 2020. Depletion of microglia in developing cortical circuits reveals its critical role in glutamatergic synapse development, functional connectivity, and critical period plasticity. *Journal of Neuroscience Research*, **98**(10): 1968–1986.
- McGuinness AJ, Davis JA, Dawson SL, Loughman A, Collier F, O'Hely M, et al. 2022. A systematic review of gut microbiota composition in observational studies of major depressive disorder, bipolar disorder and schizophrenia. *Molecular Psychiatry*, **27**(4): 1920–1935.
- Najafi AR, Crapser J, Jiang S, Ng W, Mortazavi A, West BL, et al. 2018. A limited capacity for microglial repopulation in the adult brain. *Glia*, **66**(11): 2385–2396.
- Nguyen R, Morrissey MD, Mahadevan V, Cajanding JD, Woodin MA, Yeomans JS, et al. 2014. Parvalbumin and GAD65 interneuron inhibition in the ventral hippocampus induces distinct behavioral deficits relevant to schizophrenia. *Journal of Neuroscience*, **34**(45): 14948–14960.
- Ni RJ, Gao TH, Wang YY, Tian Y, Wei JX, Zhao LS, et al. 2022. Chronic lithium treatment ameliorates ketamine-induced mania-like behavior via the PI3K-AKT signaling pathway. *Zoological Research*, **43**(6): 989–1004.
- Ni RJ, Shu YM, Wang J, Yin JC, Xu L, Zhou JN. 2014. Distribution of vasopressin, oxytocin and vasoactive intestinal polypeptide in the hypothalamus and extrahypothalamic regions of tree shrews. *Neuroscience*, **265**: 124–136.
- Ni RJ, Tian Y, Dai XY, Zhao LS, Wei JX, Zhou JN, et al. 2020. Social avoidance behavior in male tree shrews and prosocial behavior in male mice toward unfamiliar conspecifics in the laboratory. *Zoological Research*, **41**(3): 258–272.
- Oosterhof N, Kuil LE, van der Linde HC, Burm SM, Berdowski W, van Ijcken WFJ, et al. 2018. Colony-stimulating factor 1 receptor (CSF1R) regulates microglia density and distribution, but not microglia differentiation *in vivo*. *Cell Reports*, **24**(5): 1203–1217. e6.
- Smith BL, Laaker CJ, Lloyd KR, Hiltz AR, Reyes TM. 2020. Adolescent microglia play a role in executive function in male mice exposed to perinatal high fat diet. *Brain, Behavior, and Immunity*, **84**: 80–89.
- Svoboda J, Stankova A, Entlerova M, Stuchlik A. 2015. Acute administration of MK-801 in an animal model of psychosis in rats interferes with cognitively demanding forms of behavioral flexibility on a rotating arena. *Frontiers in Behavioral Neuroscience*, **9**: 75.
- VanRyzin JW, Arambula SE, Ashton SE, Blanchard AC, Burzinski MD, Davis KT, et al. 2021. Generation of an Iba1-EGFP transgenic rat for the study of microglia in an outbred rodent strain. *eNeuro*, **8**(5): ENEURO.0026–21.2021.
- Vichaya EG, Malik S, Sominsky L, Ford BG, Spencer SJ, Dantzer R. 2020. Microglia depletion fails to abrogate inflammation-induced sickness in mice and rats. *Journal of Neuroinflammation*, **17**(1): 172.
- Volk DW. 2017. Role of microglia disturbances and immune-related marker abnormalities in cortical circuitry dysfunction in schizophrenia. *Neurobiology of Disease*, **99**: 58–65.
- Walther S, Stegmayer K, Federspiel A, Bohlhalter S, Wiest R, Viher PV. 2017. Aberrant hyperconnectivity in the motor system at rest is linked to motor abnormalities in schizophrenia spectrum disorders. *Schizophrenia Bulletin*, **43**(5): 982–992.
- Warden AS, Wolfe SA, Khom S, Varodayan FP, Patel RR, Steinman MQ, et al. 2020. Microglia control escalation of drinking in alcohol-dependent mice: genomic and synaptic drivers. *Biological Psychiatry*, **88**(12): 910–921.
- Wegrzyn D, Juckel G, Faissner A. 2022. Structural and functional deviations of the hippocampus in schizophrenia and schizophrenia animal models. *International Journal of Molecular Sciences*, **23**(10): 5482.
- Yang Y, Eguchi A, Wan XY, Chang LJ, Wang XM, Qu YG, et al. 2023. A role of gut-microbiota-brain axis via subdiaphragmatic vagus nerve in depression-like phenotypes in *Chrm7* knock-out mice. *Progress in Neuro-Psychopharmacology and Biological Psychiatry*, **120**: 110652.
- Yang Y, Ishima T, Wan XY, Wei Y, Chang LJ, Zhang JC, et al. 2022. Microglial depletion and abnormalities in gut microbiota composition and short-chain fatty acids in mice after repeated administration of colony stimulating factor 1 receptor inhibitor PLX5622. *European Archives of Psychiatry and Clinical Neuroscience*, **272**(3): 483–495.
- Yao W, Cao QQ, Luo SL, He LJ, Yang C, Chen JX, et al. 2022a. Microglial ERK-NRBP1-CREB-BDNF signaling in sustained antidepressant actions of (R)-ketamine. *Molecular Psychiatry*, **27**(3): 1618–1629.
- Yao ZY, Li XH, Zuo L, Xiong Q, He WT, Li DX, et al. 2022b. Maternal sleep deprivation induces gut microbial dysbiosis and neuroinflammation in offspring rats. *Zoological Research*, **43**(3): 380–390.
- Yegla B, Boles J, Kumar A, Foster TC. 2021. Partial microglial depletion is associated with impaired hippocampal synaptic and cognitive function in young and aged rats. *Glia*, **69**(6): 1494–1514.
- Zhang K, Yang C, Chang LJ, Sakamoto A, Suzuki T, Fujita Y, et al. 2020. Essential role of microglial transforming growth factor- β 1 in antidepressant actions of (R)-ketamine and the novel antidepressant TGF- β 1. *Translational Psychiatry*, **10**(1): 32.
- Zhang L, Shirayama Y, Iyo M, Hashimoto K. 2007. Minocycline attenuates hyperlocomotion and prepulse inhibition deficits in mice after administration of the NMDA receptor antagonist dizocilpine. *Neuropsychopharmacology*, **32**(9): 2004–2010.
- Zhao XF, Alam MM, Liao Y, Huang TT, Mathur R, Zhu XJ, et al. 2019. Targeting microglia using Cx3cr1-Cre lines: revisiting the specificity. *eNeuro*, **6**(4): ENEURO.0114–19.2019.